Domain wall induced switching of whisker-based tunnel junctions

R. Schäfer,[1] R. Urban,[2] D. Ullmann,[3] H. L. Meyerheim,[3] B. Heinrich,[2] L. Schultz,[1] and J. Kirschner[3]
[1]*IFW-Dresden, Helmholtz-Strasse 20, D-01069 Dresden, Germany*
[2]*Simon Fraser University, Burnaby, BC, Canada V5A1S6*
[3]*MPI für Mikrostrukturphysik, Weinberg 2, D-06120 Halle, Germany*
(Received 25 October 2001; published 20 March 2002)

The magnetization behavior of a single-crystalline [Fe-whisker/MgO (20 ML)/Fe-film (20 ML)] sandwich (ML denotes monolayer) was studied by depth-selective Kerr microscopy. Residual stray fields of the whisker domain walls were identified to be responsible for complex magnetization processes in the iron film. A 180° wall in the whisker magnetizes the film transversally to the wall direction, depending on the internal rotation alignment of the whisker wall and not on its surface rotation. We also found that 360° walls can be formed in the film for pure topological reasons if Néel walls of certain rotation alignments are facing each other.

DOI: 10.1103/PhysRevB.65.144405 PACS number(s): 75.60.Ch, 75.70.Kw, 75.70.Cn

I. INTRODUCTION

Ferromagnetic films, separated by a nonmagnetic spacer layer that modifies or interrupts the exchange interaction, can be magnetically coupled by a number of mechanisms. Metallic interlayers in the nanometer thickness range may lead to an indirect antiferromagnetic exchange coupling,[1] a coupling that oscillates between ferro- and antiferromagnetic depending on the interlayer thickness,[2] and to nonlinear modes of coupling.[3,4] A parallel alignment of the magnetic films (weak ferromagnetic coupling) may also be caused by the ''orange peel'' effect,[5] both for insulating and metallic spacer layers. This so-called Néel type coupling is due to dipolar fields if there is a correlated interface roughness and if the interlayer is thin compared to the amplitude of the surface corrugations of the magnetic films. In patterned multilayer elements, stray fields at the edges may favor an antiparallel alignment of the magnetic films. But even in multilayers that are nominally decoupled, local dipolar interactions may occur. Magnetic charges in a magnetic layer can be matched by opposite charges in the neighboring layer.[6,7] This is achieved by superimposed, low-energy Néel walls that rotate in opposite directions in neighboring films, or by 0° quasiwalls that match the charges of 360° walls in double films (see Chap. 5.5.7 in Ref. 8 for an overview of such effects).

Recently, Parkin and co-workers discovered a related interaction:[9,10] in a trilayer system, in which hard and soft ferromagnetic layers are interspaced by a nonmagnetic layer, the hard layer can be demagnetized in magnetic fields much smaller than its coercive field, when these fields are used to repeatedly switch the magnetization of the adjacent soft magnetic layer. The demagnetization is caused by the fringing fields of *Néel walls* in the soft layer, which easily exceed several thousands A/cm. The decay of the remanent moment of the hard layer is undesired in the application of soft/hard magnetic multilayers in magnetoresistive sensors or memory cells based on the giant and tunneling magnetoresistance effects.[11,12]

In this article we report on the direct observation of such a domain wall fringing field coupling effect. As opposed to the effect mentioned before,[9,10] it is found for *Bloch walls* in iron whiskers in our case. Although such walls are expected to be largely stray-field-free by forming a two-dimensional vortex structure,[8] residual wall fringing fields at the surface can cause the switching of an iron film that is deposited in close distance to the whisker surface, separated by a nonmagnetic MgO spacer layer.

The Fe-whisker/MgO/Fe-film system is expected to provide a model system for studying the mentioned tunneling magnetoresistance effect (TMR), a spin-dependent tunneling between ferromagnetic electrodes separated by insulating oxide barriers that is of current interest for applications in magnetic random access memories and field sensors.[13] For perfect Fe/MgO/Fe junctions, a TMR of several hundred percent has been predicted due to band-structure effects.[14] The almost ideal (100) surface of an iron whisker allows the epitaxial growth of perfect films and thus enables the study of intrinsic tunneling properties.[15] A requirement for tunneling experiments is an independent switching of whisker and film, allowing one to obtain parallel and antiparallel relative magnetizations at best. The question of how remagnetization occurs in our system was the motivation for the studies presented in this paper. As will be elaborated, we in fact found possibilities to get noncollinear magnetic moments in whisker and film. Also a remarkable TMR effect was measured in preliminary experiments, but further investigations have to be carried out to get reproducible results.

II. EXPERIMENT

A. Sample preparation

Rectangular iron whiskers with (100) facets, a length between 3 and 10 mm, and a width of 100 to 300 μm were grown by chemical reaction from the vapor phase.[16] A microscopically selected surface was cleaned in ultrahigh vacuum by argon sputtering and annealing until sharp low-energy electron diffraction (LEED) and reflection (RHEED) patterns were obtained. Scanning tunneling microscopy revealed flat surfaces with atomic terraces of about 3 μm width.

After whisker preparation, single-crystal epitaxial tunnel junctions, consisting of a MgO barrier layer, an Fe top electrode, and a 20-monolayer- (ML) thick protection layer of Au were deposited at room temperature by means of molecular

beam epitaxy at a rate of 1 ML per minute. Crystallinity was maintained through the whole growth of the multilayer structure, with the (100) iron film having the same orientation as the whisker surface. Details of the sample preparation are published elsewhere.[17] The domain observations presented below were made on a sample where the MgO and Fe films were each 20 ML thick.

B. Depth-selective Kerr microscopy

The magnetic domains of the whisker and Fe film were observed separately by depth-selective Kerr microscopy.[18] This procedure relies on the magnetic information depth of the Kerr effect, which is about 20 nm in metals.[19] So for our whisker/film system there will be contrast contributions from both whisker and iron film, which will be superimposed in one image under regular microscopical conditions.

For depth selectivity, the *phase* of the Kerr amplitude has to be adjusted by using a rotatable compensator (e.g., a quarter-wave plate), located between the polarizer and analyzer in the Kerr microscope. By proper phase setting, light from selected depth zones can be made invisible if their Kerr amplitude is adjusted out of phase with respect to the regularly reflected light. Depending on the compensator setting, the whisker and film domains can so be imaged separately. For our whisker/film system the compensator adjustment for selectivity is easy because the whisker domains and their expected contrast are well known. In all images shown, the domain contrast was electronically enhanced by a standard difference image procedure in which an image of the saturated state is subtracted from an image containing domain contrast.

III. RESULTS AND DISCUSSION

A. Domain and wall structure of an (uncoated) iron whisker

The magnetic domains of iron whiskers have been intensively studied by the Bitter technique some 40 years ago (see Ref. 20 for a review). The magnetic ground state of a whisker with (100) side surfaces after demagnetization in an alternating magnetic field, observed by Kerr microscopy from two sides, is shown in Fig. 1(a). It typically consists of 180° domains along the whisker axis that may be interrupted by 90° diamond domains, depending on domain nucleation during the previous field history.[21] The zigzag wall on the side surface is actually the intersection of the two subsurface 90° walls of the diamond domain, which are folded for energetic reasons.[8] This wall is called the V line for its V-shaped internal structure.[22]

The 180° domain wall along the whisker axis is a so-called vortex wall.[8] This wall type, which was first explored theoretically by Hubert,[23] typically occurs in thick soft magnetic materials and is derived from the asymmetric Bloch wall of thick magnetic films.[24–26] As schematically shown in a cross-sectional view in Fig. 1(b), the vortex wall appears like a common Néel wall with in-plane rotation right at both surfaces, whereas in the volume the magnetization rotates parallel to the wall plane as in a classical Bloch wall. By forming vortices close to the surfaces, stray fields are

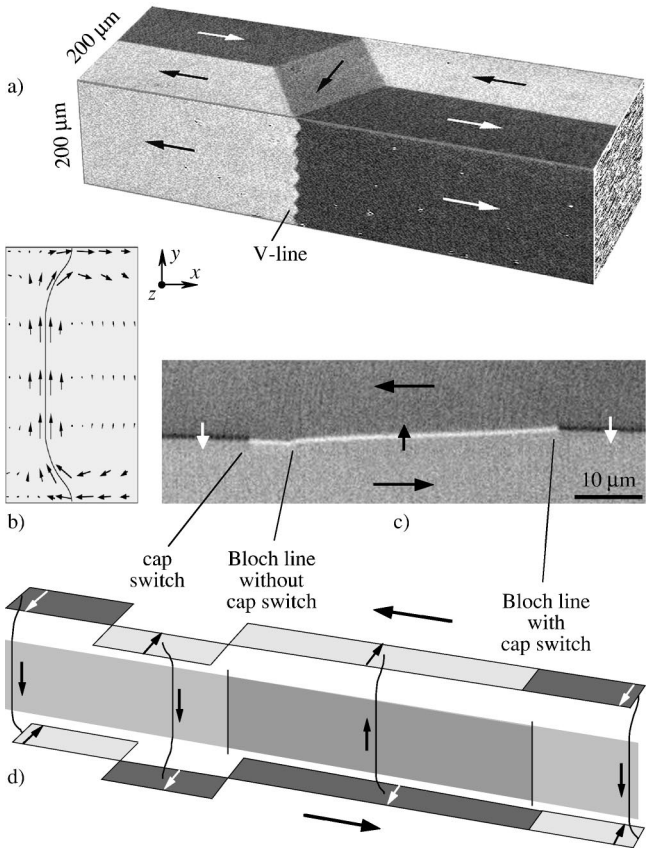

FIG. 1. Domains and domain walls in an uncoated (100) iron whisker. (a) Domain ground state, imaged by digitally enhanced Kerr microscopy. Images of neighboring sides were combined to give a perspective view. (b) Cross-sectional view of a vortex wall (schematically). Shown is the projection of the magnetization vector onto the cross section. The contour line indicates the center of the wall, i.e., the surface on which the z component passes through zero. (c) Kerr image of a 180° vortex wall on a whisker. (d) Schematics of the three types of wall transitions (after Ref. 33). The shift of the Néel cap is explained by the asymmetric wall profile under the assumption that the Bloch parts of all segments are aligned within one plane.

avoided or at least reduced, depending on the relative size of anisotropy. For materials with $Q \ll 1$ the wall is completely free of magnetic charges [the quality factor $Q = K/(J_s^2/2\mu_0)$ is defined as the ratio of anisotropy to stray-field energy, where K is the anisotropy constant and J_s is the saturation magnetization in tesla]. With increasing Q, charge reduction by vortex formation continuously diminishes until the wall will assume a one-dimensional Bloch character all through for high-Q materials.

For iron the Q factor is about 0.02. Therefore the vortex character of a wall in thick iron films or bulk crystals (such as sheets or whiskers) is expected to be well pronounced. This could in fact be confirmed experimentally by a number of surface observations using Kerr microscopy[8,27] or spin-polarized scanning electron microscopy (SEMPA).[28–30] However, the stray-field reduction at the surface of an iron wall seems to be incomplete. This is already suggested by the fact that 180° and 90° domain walls of bulk iron crystals

strongly attract the particles of a Bitter colloid.[22] Another indication is given by numerical micromagnetic calculations of iron walls. Although they were usually performed for iron films in the micrometer thickness range rather than for bulk crystals,[31,32] a small magnetization component perpendicular to the surface was found when the wall meets the surface, despite the overall vortex wall structure. This component may point in- or outwards, depending on the internal rotation orientation of the Bloch part. Also SEMPA observations of walls on iron sheets were explained in terms of a small out-of-plane component.[30] The presence of a perpendicular magnetization component at domain walls and the resulting stray magnetic field is essential for the interpretation of our observations presented below.

A high-resolution Kerr image of the main 180° wall of an uncoated whisker is presented in Fig. 1(c). The wall contrast is due to the in-plane component of magnetization, mainly showing the Néel cap of the wall (note that a clear out-of-plane contrast at iron walls could not be observed by Kerr microscopy due to the superposition of Kerr and gradient contrast).[27] Néel caps of iron walls can well be resolved by Kerr microscopy, although the ''classical'' (100) Bloch wall in an extended iron sample is expected to have a width of only about 10 $(A/K_{cl})^{1/2}=210$ nm (see Ref. 8, p. 233), which is below the resolution limit of optical microscopy. Two facts are responsible for this seemingly surprising observation: (i) The observed line with a width of the order of 1 μm may appear wider than it actually is due to diffraction broadening (depending on the ratio of the true cap width to the optical resolution limit). (ii) By numerical micromagnetic calculations,[24] performed on uniaxial magnetic films with $Q=0.1$ up to a thickness of 160 $(A/K_u)^{1/2}$, it was found that the surface wall width of a vortex wall steadily increases with film thickness, whereas the interior wall approaches the classical Bloch wall width. This tendency will roughly be true also for iron walls, so that the surface wall width on the whisker can be expected to be much larger than the theoretically estimated bulk wall width.

Characteristic for the surface wall of thick iron samples are the black and white wall segments that may be shifted or tilted at transitions [see Fig. 1(c)]. They are explained by the fact that four equivalent configurations are possible for a vortex wall:[33–35] the Bloch part in the volume may rotate clock- or counterclockwise, and the same is true for the Néel cap. As all four configurations are energetically equal, they can occur within one wall. When different wall segments meet, they form Bloch lines and cap switches as schematically explained in Fig. 1(d). Bloch lines (where the rotation orientation of the Bloch part changes) are always connected with kinks at the surface.[36] This peculiar wall twisting around Bloch lines, which is well visible in Fig. 1(c), helps in deviating some of the wall flux into the domains and thus supports the surface vortex in stray field reduction.[8] Note that the Bloch part of the wall cannot be seen by Kerr microscopy. Therefore Bloch lines without cap switches can only be identified by their surface kink in an otherwise uniform wall.

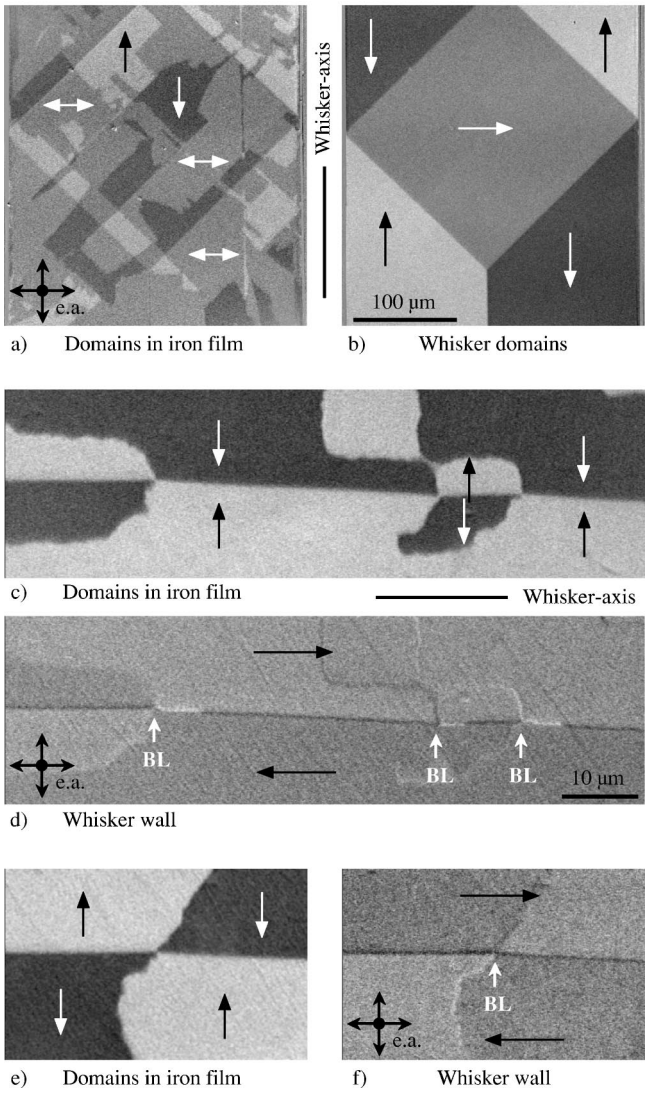

FIG. 2. Domains on the Fe-whisker/MgO (20 ML)/Fe-film (20 ML) system after ac demagnetization. The three identical patterns in (a,b), (c,d), and (e,f) were imaged selectively on whisker and film in each case.

B. Domains in the whisker/MgO/Fe-film system

Layer-selective images of the complete whisker/MgO/Fe-film system, which show identical domain patterns in whisker and iron film separately, are presented in Fig. 2. The domain states were obtained after demagnetizing the sample in an alternating magnetic field of decreasing amplitude along the whisker axis. The contrast sensitivity was along the vertical in-plane axis in all pictures, which corresponds to one of the two surface-parallel easy axes. According to crystal anisotropy, only three levels of gray are expected (as long as rotational magnetization processes are prevented in small to moderate external fields): black and white for domains magnetized along the sensitivity axis, and gray for both kinds of transverse domains. This is true for whisker and film, because the film is epitaxially grown in the same orientation as the whisker surface and thus has the same orientation of crystallographic axes.

The pattern in Figs. 2(a) and 2(b) was observed at low magnification. As compared to the simple diamond domain present in the whisker [Fig. 2(b)], the film domains [Fig. 2(a)] appear highly complex with no clear relation between film and whisker magnetization directions. This indicates the absence of significant exchange or orange peel coupling between film and whisker. Nevertheless, the diamond of the whisker is still somehow reflected in the orientation of the film domain walls. We will demonstrate below that this correlation is due to magnetostatic interaction, caused by the residual stray fields emerging from the whisker domain walls. In Figs. 2(a) and 2(b) these are the 90° walls of the diamond, which were wiggling during ac demagnetization and which thereby ''wrote'' the film domains.

In Figs. 2(c) and 2(d) a similar correlation is shown for a 180° wall running along the whisker axis. The wall, which is imaged separately in Fig. 2(d), was moving up and down during demagnetization, and by doing so, the domain pattern of Fig. 2(c) was written in the film, transferred by stray-field coupling. The black and white film domains occupy the easy axis transverse to the whisker axis in a checkerboardlike way. The presence of the 180° whisker wall is also visible in the film by a straight horizontal domain boundary line that separates ''head-on'' film domains. Interesting is the correlation between whisker wall fine structure and film domains. Those points along the straight domain boundary in the film where the checkerboard domains change contrast are obviously directly related to the presence of Bloch lines in the whisker [indicated by arrows in Fig. 2(d)], whereas pure cap switch transitions, also present in the whisker wall, have no influence. The pattern shown in Figs. 2(e) and 2(f) confirms and completes this observation. In this case the whisker wall also contains a Bloch line without a cap switch that is again related to a switch of the checkerboard domains. An interpretation of this observation will be given in Sec. III C where we will demonstrate how the checkerboard domains are formed.

The weak areal contrast in the whisker images [Figs. 2(d) and 2(f)] is most likely due to an imperfect depth selectivity in the experiment. This can also be true for the residual wall contrasts (besides that of the 180° wall). Note, however, that the Néel walls in the iron film (which surround the checkerboard domains) could also induce some charge-compensating structures in the whisker surface that could be responsible for the line contrasts in Figs. 2(d) and 2(f). We will return to this aspect at the end of Sec. III D.

C. Stray field writing of a 180° wall

The formation of the checkerboard domains can be demonstrated by following the motion of a 180° whisker wall as presented in Fig. 3. Whisker and film were initially saturated in an external field towards the right (i.e., a field along the whisker axis, which is called longitudinal direction further on). From images (a)–(c) in Fig. 3, showing the Fe-film domains, the field was inverted and continuously increased. A 180° wall, entering the image from the bottom, remagnetizes the whisker. The area of the film, which was passed by the whisker wall, remains magnetized transverse to the whisker

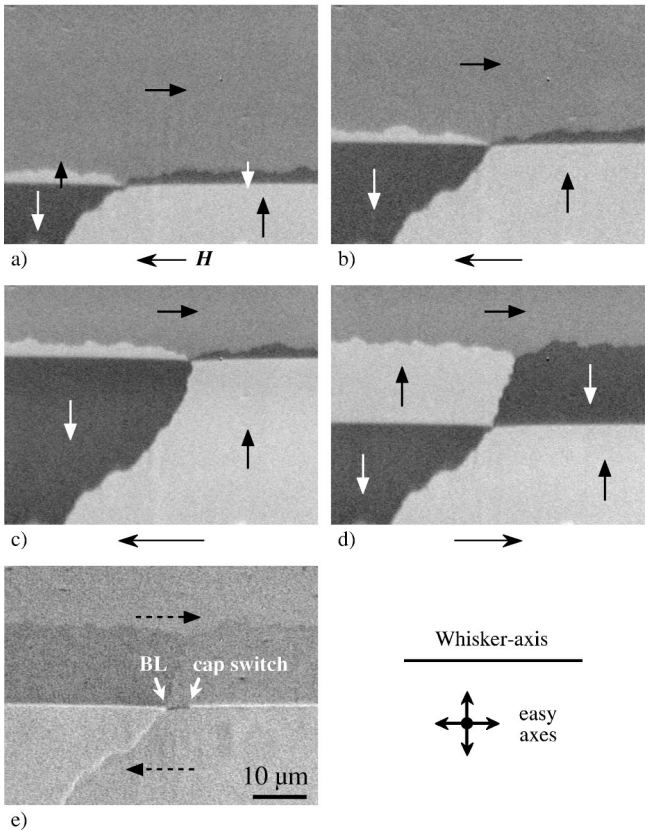

FIG. 3. Remagnetization of the iron film by motion of a 180° whisker wall in the whisker/MgO/Fe-film system. Film and whisker are imaged selectively in (a)–(d) and (e), respectively. Images (d) and (e) show identical domain states.

magnetization, either up- or downwards (white and black domains, respectively). But also in front of the moving whisker wall a narrow zone of transverse magnetization is pushed in the film. The magnetization of this front zone is opposite to that of the passed zone. When the whisker wall is moving back again in a reversed field [Fig. 3(d)], the wavy wall that separates the front zone from the nonswitched area in the film is kept in the same position as in Fig. 3(c). The withdrawing whisker wall leaves transversely magnetized film domains in the same color as the previous zones in front of the wall. A checkerboard pattern is created in this way [as in Figs. 2(c) and 2(e)].

The 180° wall in the whisker, which was responsible for the previously described process, is imaged separately in Fig. 3(e), where the same state as in Fig. 3(d) is shown. As in Fig. 2 it is immediately evident that the Bloch line (i.e., the kink) in the whisker wall is responsible for the irregular vertical (or almost vertical) checkerboard walls in the film, whereas the pure cap switch has no influence. This clearly demonstrates that the type of transverse domains in the film (up or down) does not depend on the surface rotation of the whisker wall, but on its internal rotation alignment, which changes sign across the Bloch line and which is responsible for the residual surface stray fields of the wall. Note that Bloch lines may also be shifted along the wall when a 180° wall moves. For this reason the direction of the checkerboard wall in the

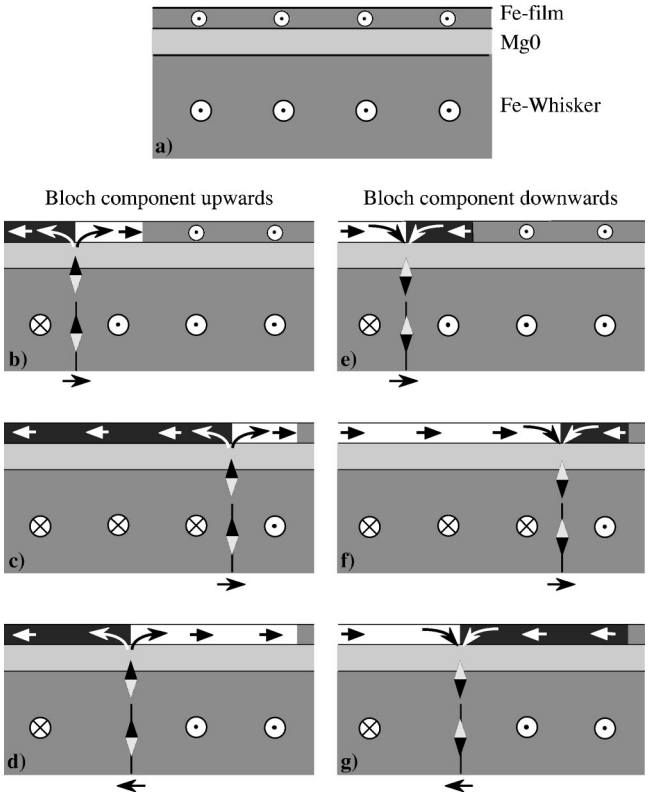

FIG. 4. Switching of the Fe film, induced by the fringing field of a moving whisker wall (schematically). Only the Bloch component of the whisker wall is considered, which has different signs in (b)–(d) and (e)–(g).

film, which indicates the position of the Bloch line, may more or less deviate from the vertical direction, depending on the position of the Bloch line during wall motion.

The diagram in Fig. 4 schematically illustrated this process of stray-field writing. Here a cross section, viewed along the whisker axis, is shown. In Fig. 4(a), whisker and film are saturated. From (b) to (c) a Bloch wall starts to remagnetize the whisker from the left [this corresponds to the states shown in the left part of Figs. 3(a)–3(c)]. Only the Bloch part of the wall is considered, because it is responsible for the surface fringing field. In the film, a black transverse domain is left behind the wall according to the wall's stray field, and a white transverse domain is pushed ahead (with a width given by the extension of the stray field). When the wall moves back to the left again (d), the white transverse domain grows at the expense of the black domain. In Figs. 4(e)–4(g) the same process is shown for a whisker wall with opposite rotation alignment, leading to opposite transverse domains in the film [this corresponds to the right-hand parts of Figs. 3(a)–3(d)]. If both rotation orientations are present within one wall, connected by a Bloch line, a checkerboard pattern is written in this way in accordance with experiments.

D. Formation of 360° walls

A further observation deserves attention. Often 360° walls are formed in the film when a 180° whisker wall moves along. They are oriented at an angle of about ±80° relative to the 180° wall direction as shown in Fig. 5(a).

The series of pictures in Figs. 5(b) and 5(c) shows a possibility how 360° walls are formed. Similar to the sequence of Fig. 3, a 180° whisker wall, entering from the bottom, pushes ahead a narrow zone of transverse magnetization in the Fe film [Fig. 5(b)]. However, this zone has two different extensions: there is a narrow regime that is separated from the nonswitched film area by a straight wall, and there is a wider regime separated by a wavy wall. When the whisker wall moves back [Fig. 5(c)], it leaves black domains in the film. They are interrupted now by 360° walls that are pulled by the whisker wall with one end being fixed at the transition points between wide and narrow domains in the upper film wall. The locations where these 360° walls occur are not connected to the structure of the whisker wall itself, because this is without Bloch lines or cap switches in this case [Fig. 5(d)].

The existence of narrow and wide perpendicular zones may be caused by the relative chiralities of the Néel walls in the iron film. To demonstrate the idea, the relevant walls together with their magnetic charges are schematically drawn in Fig. 5(e). The 180° head-on wall in the film, located above the whisker wall, may occur in two possible chiralities. Both are positively charged, caused by an underlying whisker wall with negative surface charges (in the drawing a magnetization rotation by 90° is represented by one charge unit). Also the pushed film wall can exist in two chiralities: for topological reasons, a 90° wall or a 270° wall are possible. A 270° Néel wall is assumed for the case of the narrow perpendicular zone in accordance with experiment [see white contrast at this wall in Figs. 5(b) and 5(c)] and a 90° wall in the other case.

The charge interaction between the two walls defines the possible configurations. Obviously both, the 180° head-on wall and the pushed ''head-on-side'' wall in the film are magnetized such that opposite charges are facing each other, leading to an attractive interaction between both walls. On the left, two charge units of each type are facing each other, resulting in a strong attraction between the walls. On the right there is only one negative charge in the pushed wall, leading to a weaker attraction. As the attraction is balanced by the stray field of the whisker wall, which is the same everywhere and which enforces the intermediate transverse domain, the pushed wall on the right side is further ahead than on the left.

For topological reasons, a 360° wall is formed between the transitions of both walls when the 180° wall is pulled back by the withdrawing whisker wall. So the formation of a 360° wall requires a transition in the 180° film wall for topological reasons. The existence of this transition can be verified experimentally as shown in Fig. 5(f). Here a configuration similar to that of Fig. 5(e) is imaged selectively for the film, but now with the axis of Kerr sensitivity along the whisker axis. The 180° film wall appears under these conditions. In fact, there is a wall transition at the expected location towards the left. Note that the contrast of the white segment is diminished as compared to the black segment, and also the 360° wall barely appears. This is most likely

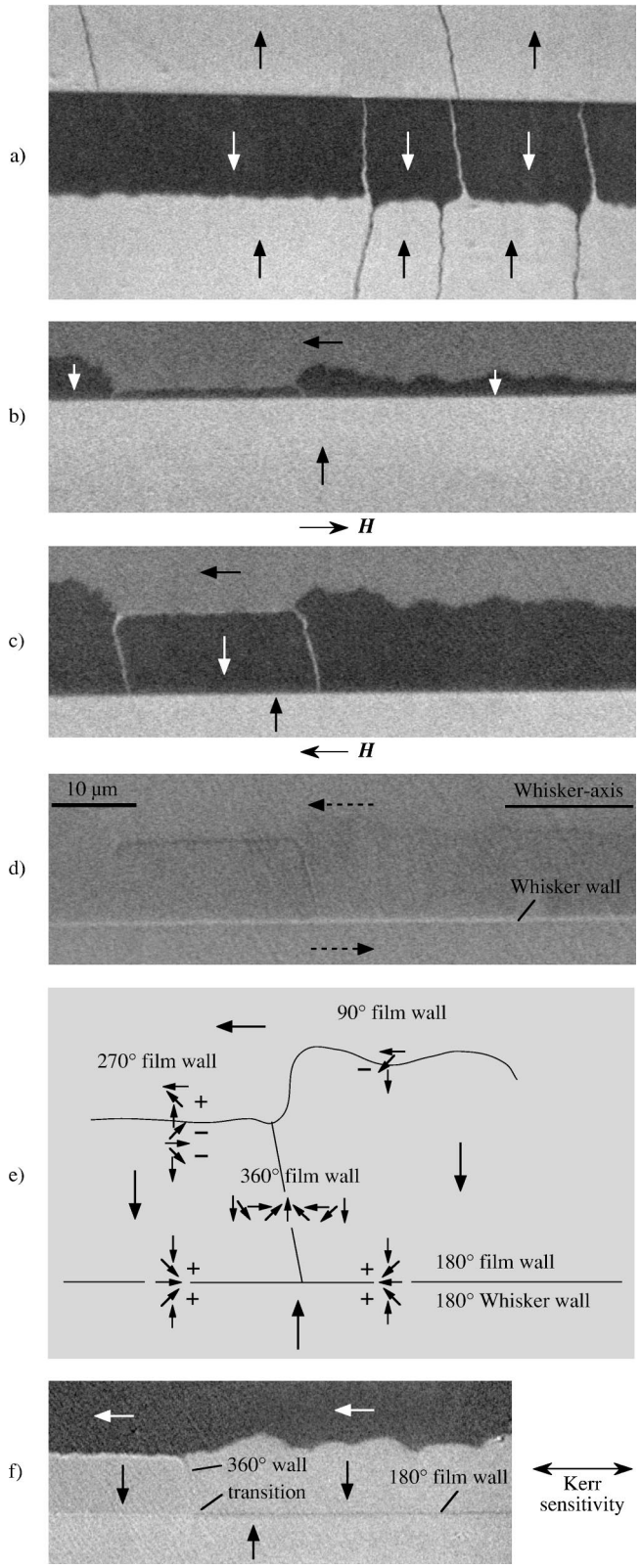

FIG. 5. (a) Domain pattern in the iron film, containing 360° domain walls. The formation of 360° walls is shown by film-selective images in (b) and (c). The domain state of (c) is selectively imaged in (d) by whisker. Wall segments of certain polarities are responsible for the formation of 360° walls as explained schematically in (e). The expected change in chirality of the 180° film wall is verified in (f).

caused by contrast contributions from the magneto-optical gradient effect, which can enhance or weaken the Kerr contrast depending on the magnetization direction[37] and which can significantly contribute to a magneto-optical image when a compensator is used. The question is whether it is the transition in the 180° film wall that induces the different chiralities in the pushed wall, or whether it is the other way around. Anyway, the occurrence of the assumed constellation may depend on field history or coincidence such as wall nucleation at the whisker edge, the previous passing of 90° whisker walls, or the previous lateral motion of Bloch lines within the 180° whisker wall.

Four facts may be noted: (i) The 360° wall is formed topologically without the pinning of a Bloch line as necessary in ordinary thin films (actually no vortices are present in the film in the configuration assumed). (ii) As the 270° pushed wall has a higher energy than the 90° pushed wall, it will occur less frequently in accordance with observations. (iii) The 180° film wall at the position of the whisker wall is a head-on wall. In pure thin films, such walls would be strongly charged and thus appear in a characteristic zigzag shape to reduce charge density.[8] This is not the case in our sample, because most of the charges at the 180° film wall are balanced by opposite charges in the underlying whisker wall. (iv) Also for the 90° and 270° film walls, charge balance could be possible to a certain degree by the formation of compensating quasiwalls in the whisker surface region. The weak line contrasts in the whisker-selective image [Fig. 5(d)] at the positions of the film walls might be an indication of such features, as already mentioned at the end of Sec. III B. Interestingly, this residual whisker contrast is stronger at the location of the 270° film wall. This could indicate a better charge compensation for 270° walls in accordance with the observed fact that the 270° wall is straight as opposed to the ragged, stronger unbalanced 90° film wall.

IV. CONCLUSIONS AND OUTLOOK

An iron film with a thickness of 20 monolayers was grown epitaxially on an iron whisker, interspaced by a 20-monolayer-thick magnesium oxide layer. The magnetization behavior of whisker and film was observed separately by depth-selective Kerr microscopy.

No significant exchange or orange peel coupling between film and whisker was found. We could demonstrate, however, that a moving 180° whisker wall acts on the Fe film by ''writing'' domains in the film that are magnetized transverse to the wall direction in accordance with crystal anisotropy. The sign of transverse domains depends on the internal rotation sense of the whisker wall, not on its surface rotation. This clearly indicates that residual fringing fields, emerging from the whisker wall, must be responsible for the interaction. We also found that 360° walls can be formed in the film if Néel walls of certain rotation orientations are facing each other. While the presence of such walls in thin films is usually connected with the pinning of Bloch lines at defects, it is caused by pure topological reasons in our samples.

Note that the existence of the expected fringing fields around walls would still have to be confirmed by micromag-

netic calculations, which are so far not available for iron walls in the thickness range of a whisker. It is also expected that the wall structure of the whisker will be modified by the presence of the iron film in close distance to the whisker surface, which again can have a mutual influence on the film. This question as well as the more intuitive arguments of charge compensation and interactions used for the explanation of several observations in this paper would require micromagnetic calculations for proof.

ACKNOWLEDGMENT

Thanks are due Manfred Rührig for critically reading the manuscript.

[1] P. Grünberg, R. Schreiber, Y. Pang, U. Walz, M. B. Brodsky, and H. Sowers, J. Appl. Phys. **61**, 3750 (1987).
[2] S. S. P. Parkin, N. More, and K. P. Roche, Phys. Rev. Lett. **64**, 2304 (1990).
[3] M. Rührig, R. Schäfer, A. Hubert, R. Mosler, J. A. Wolf, S. Demokritov, and P. Grünberg, Phys. Status Solidi A **125**, 635 (1991).
[4] B. Heinrich, J. F. Cochran, M. Kowalewski, J. Kirschner, Z. Celinski, A. S. Arrott, and K. Myrtle, Phys. Rev. B **44**, 9348 (1991).
[5] L. Néel, C. R. Hebd. Seances Acad. Sci. **255**, 1676 (1962).
[6] S. Middelhoek, J. Appl. Phys. **37**, 1276 (1966).
[7] J. C. Slonczewski, J. Appl. Phys. **37**, 1268 (1966).
[8] A. Hubert and R. Schäfer, *Magnetic Domains: The Analysis of Magnetic Microstructures* (Springer, Berlin, 1998).
[9] L. Thomas, M. Samant, and S. S. P. Parkin, Phys. Rev. Lett. **84**, 1816 (2000).
[10] L. Thomas, J. Lüning, A. Scholl, F. Nolting, S. Anders, J. Stöhr, S. S. P. Parkin, Phys. Rev. Lett. **84**, 3462 (2000).
[11] M. N. Baibich, J. M. Broto, A. Fert, F. Nguyen van Dau, F. Petroff, P. Etienne, G. Creuzet, A. Friederich, and J. Chazelas, Phys. Rev. Lett. **61**, 2472 (1988).
[12] G. Binàsch, P. Grünberg, F. Saurenbach, and W. Zinn, Phys. Rev. B **39**, 4828 (1989).
[13] J. S. Moodera and L. R. Kinder, J. Appl. Phys. **79**, 4724 (1996).
[14] W. H. Butler, X.-G. Zhang, and T. C. Schulthess, Phys. Rev. B **63**, 054416 (2001).
[15] W. Wulfhekel, M. Klaua, D. Ullmann, F. Zavaliche, J. Kirschner, U. Urban, T. Monchesky, and B. Heinrich, Appl. Phys. Lett. **78**, 509 (2001).
[16] S. S. Brenner, Acta Metall. **4**, 62 (1956).
[17] M. Klaua, D. Ullmann, J. Barthel, W. Wulfhekel, J. Kirschner, R. Urban, T. L. Monchesky, A. Enders, J. F. Cochran, B. Heinrich, Phys. Rev. B **64**, 134411 (2001).
[18] R. Schäfer, J. Magn. Magn. Mater. **148**, 226 (1995).
[19] G. Traeger, L. Wenzel, and A. Hubert, Phys. Status Solidi A **131**, 201 (1992).
[20] D. J. Craik and R. S. Tebble, *Ferromagnetism and Ferromagnetic Domains* (North-Holland, Amsterdam, 1965).
[21] B. Heinrich and R. Schäfer (unpublished).
[22] R. W. DeBlois and C. D. Graham, Jr., J. Appl. Phys. **29**, 931 (1958).
[23] A. Hubert, Z. Angew. Phys. **32**, 58 (1971).
[24] W. Rave and A. Hubert, J. Magn. Magn. Mater. **184**, 179 (1998).
[25] A. Hubert, Phys. Status Solidi **38**, 699 (1970).
[26] A. E. LaBonte, J. Appl. Phys. **40**, 2450 (1969).
[27] R. Schäfer and A. Hubert, Phys. Status Solidi A **118**, 271 (1990).
[28] H. P. Oepen and J. Kirschner, Phys. Rev. Lett. **62**, 819 (1989).
[29] M. R. Scheinfein, J. Unguris, R. J. Celotta, and D. T. Pierce, Phys. Rev. Lett. **65**, 668 (1989).
[30] O. S. Anilturk and A. R. Koymen, J. Magn. Magn. Mater. **213**, 281–292 (2000).
[31] M. R. Scheinfein, J. Unguris, J. L. Blue, K. J. Coakley, D. T. Pierce, R. J. Celotta, and P. J. Ryan, Phys. Rev. B **43**, 3395 (1991).
[32] A. Aharoni and J. P. Jakubovics, Phys. Rev. B **43**, 1290 (1991).
[33] R. Schäfer, W. K. Ho, J. Yamasaki, A. Hubert, and F. B. Humphrey, IEEE Trans. Magn. **27**, 3678 (1991).
[34] V. E. Zubov, G. S. Krinchik, and S. N. Kuzmenko, Zh. Eksp. Teor. Fiz. **99**, 551 (1991) [Sov. Phys. JETP **72**, 307 (1991)].
[35] S. Huo, J. E. L. Bishop, J. W. Tucker, W. M. Rainforth, and H. A. Davies, J. Magn. Magn. Mater. **218**, 103 (2000).
[36] S. Shtrikman and D. Treves, J. Appl. Phys. **31**, 1304 (1960).
[37] R. Schäfer, M. Rührig, and A. Hubert, Phys. Status Solidi A **145**, 167 (1994).